

2 Using vibrating-wire technology for precipitation measurements

Claude E. Duchon

School of Meteorology, University of Oklahoma, OK, USA

Table of contents

2.1	Introduction.....	33
2.2	Principles of operation.....	35
2.3	Description of field site and data acquisition.....	36
2.4	Advantages of using three vibrating wires.....	41
2.5	Calibration-verification.....	44
2.6	Temperature sensitivity.....	47
2.7	Rain rate estimation	50
2.8	Very low precipitation events	53
2.9	Summary	56
	References.....	58

2.1 Introduction

Vibrating-wire technology applied to the measurement of precipitation was developed at the Norwegian Geotechnical Institute (NGI), Oslo in the early 1980s (Bakkehøi et al. 1985). This application was an outgrowth of previous work at NGI involving the design and manufacture of instruments employing the vibrating-wire technique to measure strain and loads in concrete in bridges, earth pressures in dams, soil porewater pressure in boreholes under embankments and other geomechanical examples (Tunbridge and Øien 1988). The vibrating-wire precipitation gauge that has been available for many years is called the NGI Geonor T-200B and is the gauge investigated in this Chapter. Figure 1 is an example of a T-200B with and without its case removed. The Geonor T-200B gauge is in the class of a weighing-recording gauge and is widely

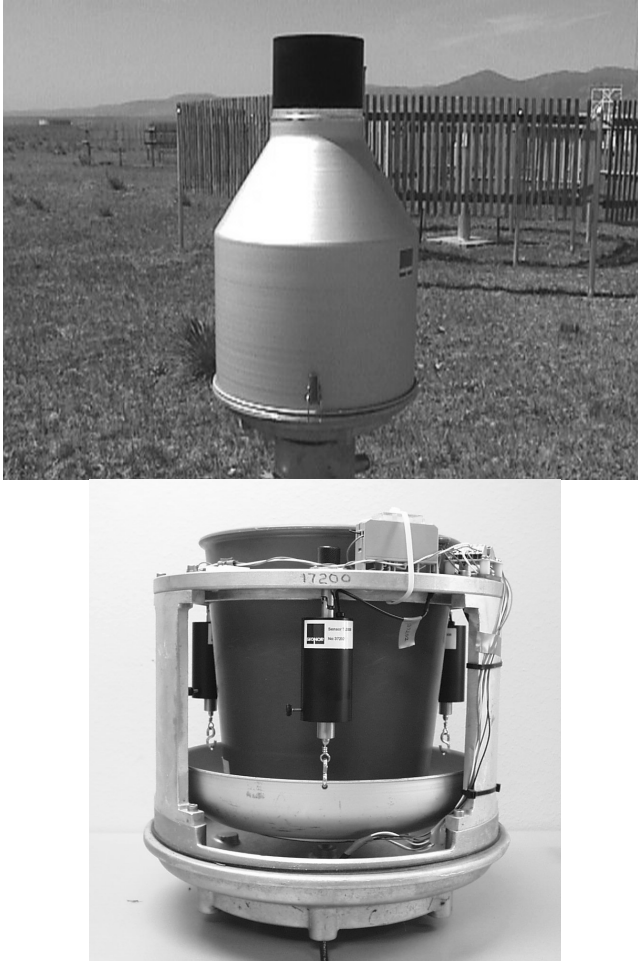


Fig. 1. A Geonor T-200B in the field (*upper*) and with its case removed (*lower*). The 12 L bucket rests in a support dish suspended from a circular flange by three vibrating wire transducers. Maximum precipitation capacity of the bucket is 600 mm (24 in)

used at more than 1400 locations world-wide of which over 500 are in Canada and the United States (Brylawski 2007, personal communication).

The purpose of this Chapter is to provide a summary of various field investigations involving the Geonor gauge that have been performed since 2000, mainly at Norman, Oklahoma, USA. The summary begins with a review of the essentials of gauge operation. This is followed by six Sections dealing with, in order, a description of the

measurement site and data acquisition, advantages of using three versus two or one vibrating wires, calibration-verification of the wires, sensitivity of vibrating wire frequency to temperature, comparison of rain rates from the Geonor to rain rates from a disdrometer and observations of very low precipitation events. The last Section highlights the findings. This Chapter deals only with liquid precipitation, the primary reason being that frozen precipitation typically occurs only a few times annually in central Oklahoma and usually in the form of sleet or freezing rain. In addition, the gauge is unheated and, as will be seen later, its orifice is at ground level.

2.2 Principles of operation

The basis of operation of the Geonor vibrating wire precipitation gauge is that the fundamental resonant frequency of a wire secured at one end and under tension at the other end is given by

$$f = \frac{1}{2L}(T/u)^{1/2} \quad (1)$$

where f is frequency, L is length of the wire, T is tension and u is mass per unit length of wire. The derivation of Eq. (1) is given by Raichel (2006, p. 71). Tension is supplied by the weight of the bucket and its contents.

As shown by Bakkehøi et al. (1985), the relationship between the fundamental resonant frequency of the wire and the strain on the wire is

$$f^2 - f_0^2 = K \frac{\varepsilon E g}{4L^2 \rho} \quad (2)$$

where ε is strain, E is Young's modulus, g is acceleration due to gravity, ρ is density of the wire, f is frequency of vibration at strain ε , f_0 is the frequency at zero strain and K is a constant of proportionality dependent on the design of the gauge.

However, Lamb and Swenson (2005) pointed out that if there is zero strain, the null frequency also must be zero. To remedy this situation, they consider f_0 to be a reference frequency at some reference strain ε_0 determined by the weight of the empty bucket and/or the bucket support. Ignoring a change in length of the wire in Eq. (2) from reference strain to the applied strain, the appropriate expression for frequency related to strain is

$$f^2 - f_0^2 = K \frac{(\varepsilon - \varepsilon_0) E g}{4 L^2 \rho} \quad (3)$$

Given that constant E is the ratio of stress T/A to strain, where A is the cross-sectional area of the wire, it follows that

$$f^2 - f_0^2 = K \frac{(T - T_0) g}{4 L^2 \rho A} = K \frac{(T - T_0) g}{4 L^2 u} \quad (4)$$

The differential tension $T - T_0$ is a consequence of the weight W of the contents in the bucket (or contents plus bucket). Recognizing that tension is a reactive force on the wire, i.e., $T - T_0 = Wg$, Eq. (4) becomes

$$f^2 - f_0^2 = K \frac{Wg^2}{4 L^2 u} \quad (5)$$

We see that the relation between precipitation (as embedded in W) and frequency of a vibrating wire is nonlinear.

While Eq. (5) is valid, the actual formulation used by Geonor in calibrating vibrating wires captures the nonlinearity in the form of a second-degree polynomial given by

$$P = A(f - f_0) + B(f - f_0)^2 \quad (6)$$

in which P is the depth of the precipitation in appropriate units consistent with the units of constants A and B . Figure 2 shows a plot of each term in Eq. (6) for a typical vibrating wire. The linear term controls the accumulation P near empty bucket while near full bucket the contributions from the linear and square terms are about equal.

2.3 Description of field site and data acquisition

The data used in the various analyses in this Chapter were acquired from a field site located on the north campus of the University of Oklahoma, Norman (97.465° W, 35.236° N) that has good exposure in all directions. Figure 3 shows the pit from which all Geonor measurements were taken.

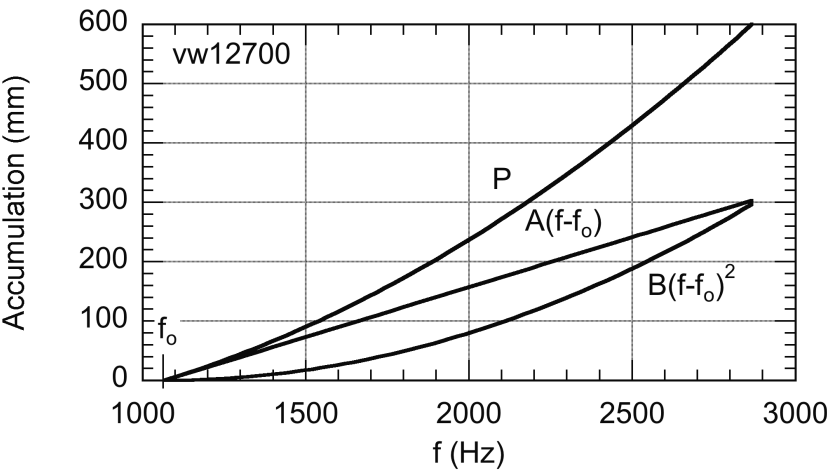


Fig. 2. Typical plot of precipitation accumulation versus frequency from Eq. (6) showing contributions from linear and nonlinear terms

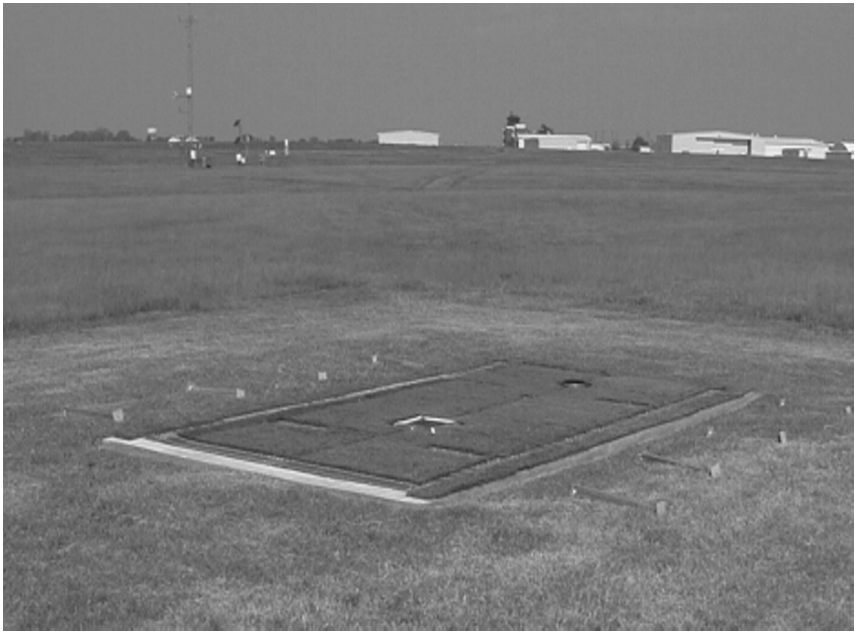


Fig. 3. View of pit with Geonor orifice at far end and 2dvd orifice at near end

The pit has interior dimensions $3.7 \text{ m} \times 1.8 \text{ m} \times 1.4 \text{ m}$ deep and is covered by a grill to which is attached a fabric to prevent splashing of raindrops. The Geonor is located at the far end of the pit and its orifice is about 1 cm above the fabric. A two-dimensional video disdrometer (2dvd) is located at the near end of the pit and its orifice is also about 1 cm above the fabric. Figure 4 shows the interior of the pit with the Geonor at the near end and the 2dvd and supporting electronic equipment at the far end. The 2dvd was designed and constructed by Joanneum Research, Graz, Austria. More will be said about the disdrometer in Sect. 2.7.

All data were collected using a Campbell Scientific, Inc., 23X data logger. One-minute averages of wind speed and wind direction near the pit at a height of 2 m, air temperature inside the Geonor case close to a vibrating wire transducer, air temperature inside the pit near the Geonor, data logger temperature, data logger voltage, frequencies from each vibrating wire and their conversion to accumulation of precipitation in units of millimeters were transmitted from the site to the University of Oklahoma and archived on disk.

There are two instructions in the data logger available to determine the frequency of each vw (vibrating wire). The P3 instruction counts the integer number of cycles over a selected time interval using a pulse counting method. The result is that the frequency is accurate to within ± 1 pulse (cycle) over the given time interval. For 1-minute averaging the inaccuracy is within $\pm 1 \text{ cycle}/60 \text{ s} = \pm 0.0166 \text{ Hz}$ which is equivalent to the resolution in frequency and is independent of frequency. However, because of the quadratic relation in Eq. (6), there is a linear relation between error in accumulation with frequency due to error in frequency. For a typical vw the results are: $\pm 0.0166 \text{ Hz} = \pm 0.003 \text{ mm}$ for empty bucket and $\pm 0.0166 \text{ Hz} = \pm 0.008 \text{ mm}$ for full bucket.

The P27 instruction calculates the time required to count a fixed number of cycles so that the ratio of the latter to the former is the frequency of the vw. The P27 instruction was used most often with its control parameters set such that 3000 cycles were required to occur within 3 s for each vw and the procedure repeated every 10 s. Thus, in successive 10 s increments 9 s were available for measurements of frequency from the three vws and 1 s for all other meteorological data. Six successive measurements for each variable were averaged to yield the 1-minute data used in all subsequent analyses.



Fig. 4. View of inside of pit with Geonor in foreground and 2dvd in background

The P27 instruction produces a smoother accumulation time series than the P3 instruction when rain rates are small. Figures 5a and 5b show a low intensity rain event over a 2-hour period beginning about minute 760 and ending at minute 870. Figure 5c shows the subsequent hour in which there is no precipitation. The standard deviation of the differences in Fig. 5c, in which there is no rain, reflects mainly the resolution error in the P3 instruction. Because the standard deviations in Figs. 5a and 5b are approximately the same as the standard deviation in Fig. 5c, the conclusion is that instruction P27 yields a better estimate of rain rate than instruction P3. The larger fluctuations using instruction P3 relative to P27 also can be visually observed in each panel.

Just the opposite conclusion follows when rain rates are high. Figure 6a is an example of very high rain rates concentrated around minute 1410. Note that the P3 time series has been shifted by 1 minute so that the individual rain rates can be easily distinguished. Because of the insensitive scale, the rain rates appear to be virtually identical. However, Fig. 6b, in which the time series of differences is plotted (without the time shift), shows that differences as large as 10 mm/h can be observed. The differences arise because of the nonlinear changes in

rain rate during the course of a minute. Instruction P3 samples continuously in time while instruction P27 computes the time needed to count 3000 cycles six times per minute, which, at full bucket, is about 6.3 s (see Fig. 2).

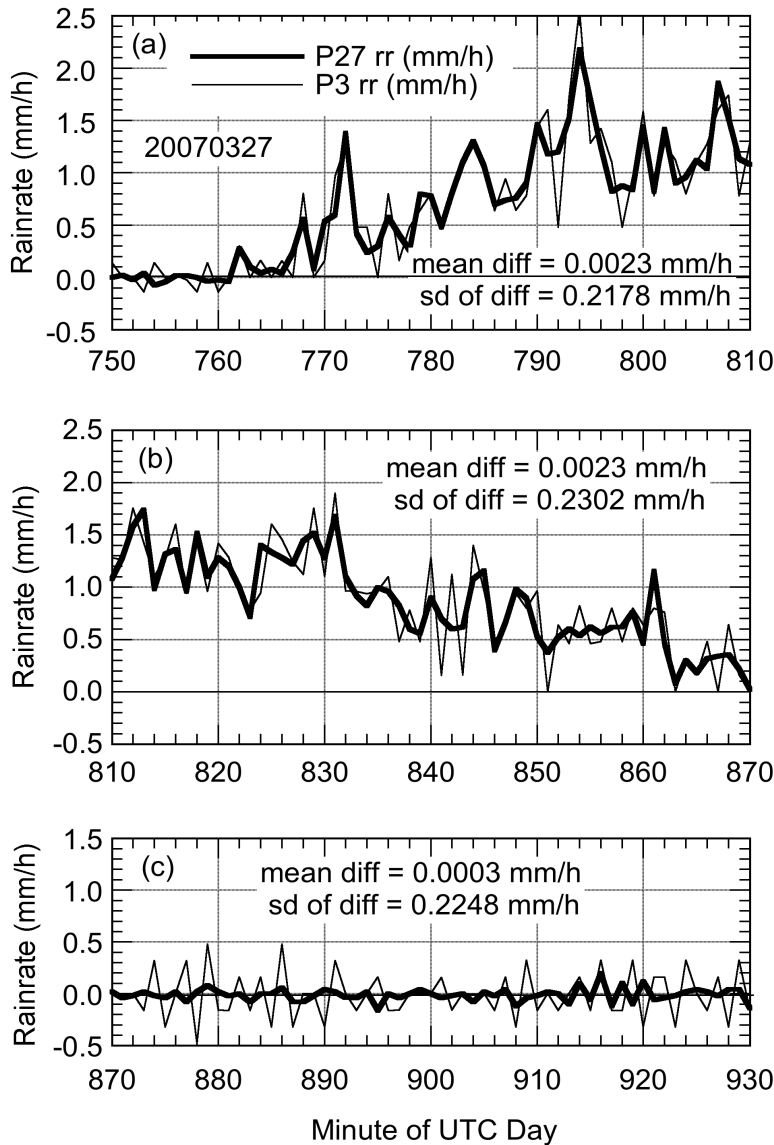


Fig. 5. Comparison of time series from instructions P3 and P27 for low 1-minute rain rates. (a) First 60 minutes, increasing rain rate. (b) Second 60 minutes, decreasing rain rate. (c) Third 60 minutes, zero rain rate

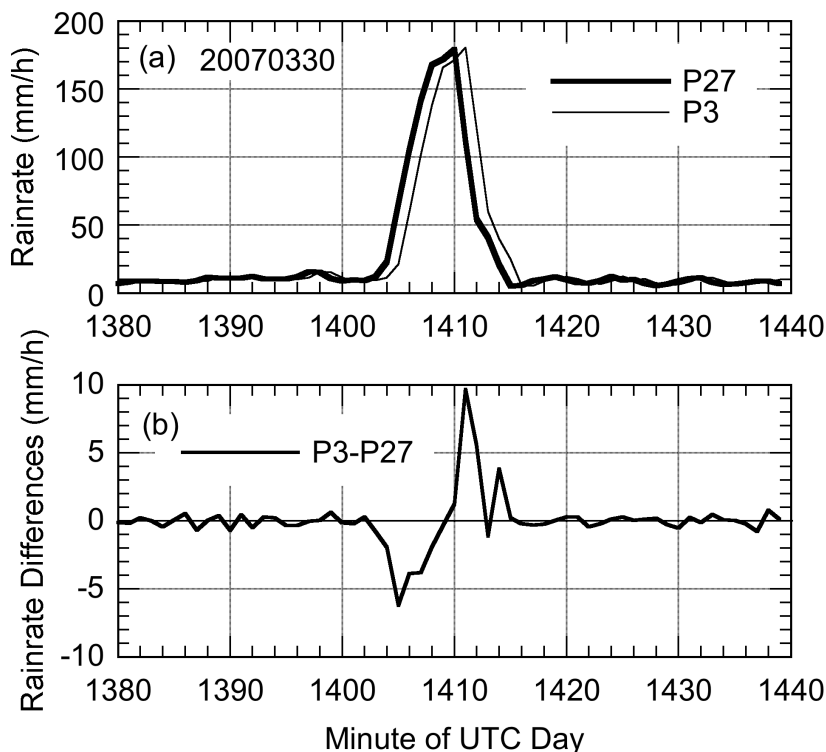


Fig. 6. (a) Rain rates using instruction P27 and P3 for an intense rainfall event. (b) Differences in rain rate using P27 and P3

In summary, instruction P27 is better for estimating low rain rates than instruction P3 because of its higher resolution in frequency, while at higher rain rates P3 is better because it samples continuously with time thereby accommodating nonlinear changes in rain rate during the course of a minute. Both instructions yield the same accumulations of precipitation with time.

2.4 Advantages of using three vibrating wires

The Geonor T-200B can operate with one, two, or three wires. In the case of using one or two wires, the remaining suspension is provided by two chains or one chain, respectively. Apart from the cost of transducers, the advantage lies in using three wires. With three wires, a continuous comparison between pairs of wires is available that can be

used to determine if and when the performance of a wire warrants replacement. If that occurs, the remaining two and a chain can be used to provide continuous measurements of accumulation. Also, and particularly for low rain rate estimation and high wind speed, the average of the accumulations from three wires yields better estimates than employing only one wire. As air passes over the inlet orifice, the air pressure inside the case is reduced (the Bernoulli effect). The gustiness in the wind produces a variable pressure on the suspended bucket resulting in variable tension on the wires and fluctuations in their natural frequency. By averaging the three outputs, noise due to the wind is significantly reduced and the best estimate of accumulation retained.

Figure 7 is an example that demonstrates the value of averaging. Each of the five time series (a) through (e) shows the residuals or departures (in mm) from a smooth curve fitted to each time series of accumulation (not shown) over a period of 2 hours with no precipitation. The residuals are equivalent to the fluctuations in 1-minute accumulations. The top three time series show simultaneous residuals for a mean wind speed of 3.94 m/s at 2 m and an accumulation of 98 mm. Their standard deviations vary from 0.00108 mm to 0.00141 mm. If the three accumulation time series are averaged minute-by-minute and a smooth curve fitted to the averages, the residuals are shown in time series (d). The standard deviation is 0.00073 mm, a substantial reduction of noise relative to that in any single wire. If one hypothesizes that the residuals in time series (a), (b) and (c) are white noise, then, theoretically, the variance of the average time series (d) would be 1/3 the average of the variances of the three wires, or a reduction in variance of 67%. The actual reduction is 66%.

Figure 7e shows that the higher the wind speed the greater the noise. The computation of the time series of residuals here is similar to that in time series (d) except that a different date and time have been examined in which the accumulation is only 11 mm greater but the mean wind speed is 9.11 ms^{-1} . We see that the standard deviation is five times larger than in time series (d) in which the mean wind speed is somewhat less than $\frac{1}{2}$ that in (e). Thus wind speed is the primary contributor to noise in accumulation time series in otherwise normally functioning vibrating wires. Accumulation noise is impacted also by the magnitude of the accumulation itself. In a case (not shown) in which there were 585 mm in the bucket and the mean wind speed was 4.04 ms^{-1} , the standard deviation of the residuals or fluctuations in accumulation was 0.00159 mm, more than twice that in comparable time series (d) in Fig. 7 with 98 mm accumulation. While one would expect the greater mass in the bucket to dampen the wind-induced

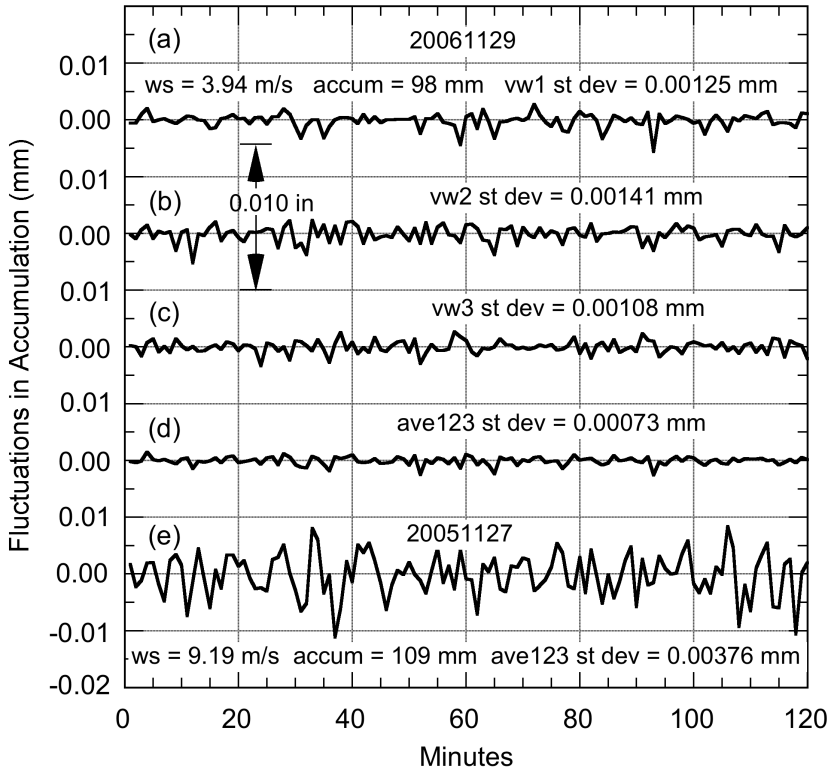


Fig. 7. (a) – (c) Noise in accumulation due to wind (~ 4 m/s at 2 m) for each of the three vibrating wires over a 2-hour period. (d) Wind noise when the accumulations from the three wires are averaged. (e) Wind noise when wind speed is somewhat more than doubled (~ 9 m/s)

fluctuations in accumulation, the change in accumulation per unit change in frequency at 585 mm accumulation is twice that at 98 mm (see Fig. 2). Apparently, the greater sensitivity of change in accumulation to change in frequency with increasing accumulation overwhelms the effect of increasing mass in the bucket.

It should be emphasized that the above analysis was based on a gauge in a pit, well protected from the wind. Any vibrations on an aboveground gauge due to the force of the wind directly on the gauge can cause fluctuations in accumulation that would be added to the noise described above.

In summary, noise in accumulation due to wind increases with both increasing wind speed and increasing accumulation in the bucket.

While this noise will not significantly affect rain or snow accumulations, it can significantly affect computation of rain and snow rates.

2.5 Calibration-verification

To monitor possible changes in coefficients A and B in Eq. (6) from their factory values, a calibration-verification (cal-ver) is performed in the field. If changes are observed based on the cal-ver, the vibrating wire transducer(s) requires recalibration. In the cal-ver procedure various known weights are placed in the bucket, the equivalent accumulations in mm of water calculated and the observed accumulations based on the frequency-to-accumulation conversion from Eq. (6) compared to the accumulations based on the weights. Fourteen stainless steel weights, each in the form of a disk with diameter 14.3 cm, thickness 0.6 cm and a hole in the center, were machined to weigh 800 g each for which the equivalent water accumulation in the bucket is 40 mm. The disks were weighed using both a precision mechanical balance and a precision electronic balance. Based on independent measurement trials, the inaccuracy of the weight of a disk was found to be within ± 0.5 g and the total weight of all disks within ± 4 g or ± 0.20 mm at 600 mm accumulation. The range in mean disk weight was from 797.5 g to 800.2 g.

The first step in a cal-ver is to sequentially place the disks onto a spindle mounted in the center of another disk made of a polymer machined to snugly fit inside the base of the bucket. Two or three 1-minute measurements were allowed for the empty bucket, spindle and mount and each added disk. Measurements were made until all 14 metal disks were stacked, followed by similar measurements after each disk and spindle and mount were removed and at empty bucket.

Results from a complete cal-ver are shown in Fig. 8. Figure 8a shows the differences between the observed or measured accumulation and the weight (in units of equivalent accumulation) versus weight. That there are two traces for each wire (vw1, vw2, vw3) and their average (ave123) is a result of successively adding all the weights and then reversing the process. This figure shows that the absolute departures from their initial values for the individual wires increase with increasing weight in the bucket, while the average differences are comparatively flat. The explanation for the diverging curves is that the center of mass becomes slightly displaced from the vertical as the disks are stacked one upon another. Thus this method of calibration-verification would not be appropriate when only one or two wires are used because compensation for displacement of the center of mass would not be taken into account.

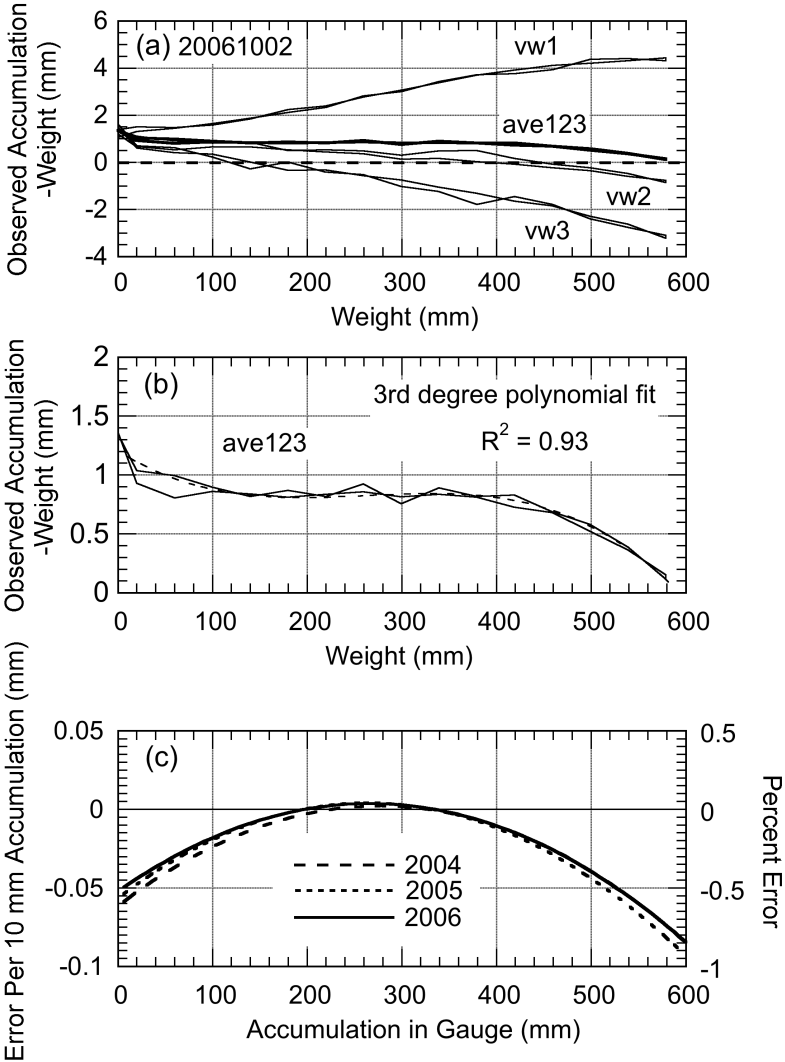


Fig. 8. (a) Differences between observed accumulation and weight in bucket (converted to accumulation) for each wire and their average. (b) As in (a) but with an expanded scale showing the best polynomial fit to the average differences. (c) Derivative of the polynomial in (b) showing error per 10 mm accumulation and percent error with accumulation. Results from previous two years are also shown

It should be noted that the mean curves for cal-vers of the same wires in 2004 and 2005 (not shown) were quite similar to that for 2006 in Fig. 8a. Although the slopes of the individual vibrating wire curves were different, their positions relative to the mean curve were the same. Given that the bucket, spindle disk and vibrating wire transducers have the same emplacement relative to each other for each cal-ver, the conclusion is that the increasing horizontal displacement of the center of mass with increasing number of weights is due to a slight offset of the spindle from vertical.

The next step in the cal-ver is to fit a smooth curve to the average differences. Figure 8b is an expanded view of the ave123 curve in Fig. 8a and includes a minimum least-squares best-fit polynomial. It is believed that the true average differences, in fact, vary smoothly with weight in the bucket and the departures from the fitted curve are measurement noise. The third step is to differentiate the polynomial. The result is shown in Fig. 8c for the polynomial in (b) and for similar polynomials from the previous two years. The curves can be interpreted as the error in accumulation per 10 mm of accumulation or percent error. A 10 mm denominator was chosen because it is a nominal amount for precipitation event totals in the Southern Great Plains. Figure 8c indicates that near empty bucket the error in a 10 mm precipitation event is about -0.05 mm or an undercatch of about 0.5%. When the bucket is around one-half full the error is close to zero and when it is completely full the error for a 10 mm precipitation event approaches -0.1 mm or an undercatch of 1%.

It is apparent that, based on these cal-vers, there has been no need to recalibrate any of the wires. That is, the values of the coefficients A and B in Eq. (6) originally provided by the factory for each wire have not significantly changed. It should be emphasized that the only purpose of a cal-ver is to assess the correctness of the coefficients in Eq. (6). The inaccuracy of a measured or observed precipitation amount depends mainly on other factors, e.g., undercatch due to wind (aboveground gauges), particularly for solid precipitation, wetting loss, evaporation or sublimation loss (negligible with continuous measurements) and splash-in or splash-out (see, for example, Groisman and Legates 1994). This investigation suggests that factory determined coefficients for vibrating wires are accurate and stable with time. The author has performed many other calibration-verifications since 2000 not only of this gauge (with different wires) but also five three-wire gauges at the National Center for Atmospheric Research, Boulder, CO, USA. To date a recalibration was recommended for only one wire and one wire broke.

2.6 Temperature sensitivity

Figure 9a shows an example of the strong inverse relation between accumulation and gauge temperature that can be easily observed on days with a smoothly varying diurnal oscillation in air temperature. The temperature fluctuations between minute 360 and minute 840 (6 pm and 8 am local time) are a consequence of the corresponding fluctuations in 2-m wind speed shown in Fig. 9b with a steep temperature inversion. The data from the two curves in Fig. 9a were used to produce a plot of accumulation versus gauge temperature as shown in Fig. 10a. After applying a least-squares linear fit to these data, the result is the dashed line, the slope of which is the temperature coefficient that, for this example, has the value $-0.0901 \text{ mm}/10^\circ\text{C}$ or approximately 0.1 mm per 10°C .

Plots similar to that in Fig. 10a were created for each suitable day for each wire and their average (ave123) between 17 January 2003 and 7 April 2007. The resulting temperature coefficients are shown in Fig. 10b. The solid line is the minimum least-squares linear fit to the data (the circles) beginning 11 October 2003, the beginning date from which the same wires have been in continuous use. There is considerable scatter of the individual temperature coefficients, but, with an R-squared value of 0.94, the linear change of temperature coefficients with accumulation is clearly significant. The greater the accumulation in the bucket, the more negative the temperature coefficient – by a factor of four from empty bucket to full bucket. Approximately one-third of the available days provided an acceptable accumulation-gauge temperature plot from which a temperature coefficient could be calculated. The remaining days had precipitation, a frontal passage, too small a diurnal temperature range, or other weather phenomena that produced complicated diurnal variations in temperature. Comparatively few days showed the ideal highly eccentric ellipse-like variation in Fig. 10a or the near 1:1 temperature – accumulation relation in Fig. 9a.

Temperature coefficients were calculated also for each wire. The labeled dashed lines in Fig. 10b are their minimum least-squares linear fits. If the supporting data for the dashed lines were plotted, the scatter of points for each wire would be larger than that for the average or solid line. As Fig. 10b shows, each wire has its own characteristic variation of temperature coefficient with accumulation.

The impact of the sensitivity of transducer frequency to temperature occurs during precipitation. Typically, temperature decreases during a precipitation event, particularly at the onset. Assuming a drop in

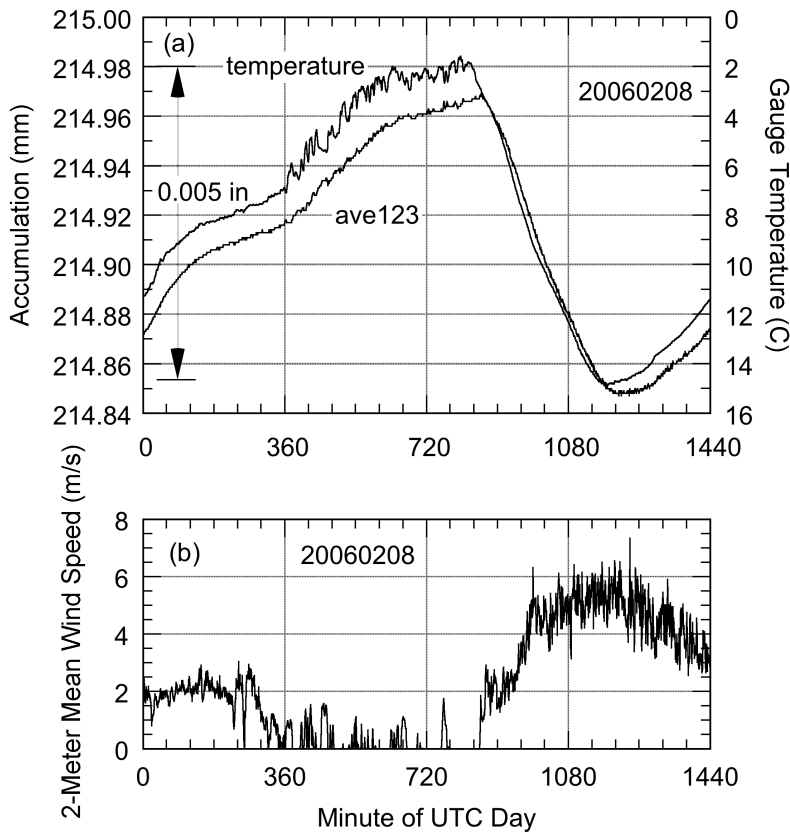


Fig. 9. (a) An example of the relationship between apparent accumulation and gauge temperature. (b) Associated 2-m wind speed

temperature of 10°C, an initial accumulation of 200 mm and a true 10 mm precipitation event, the overestimate would be about 0.1 mm or 1%. For a true 1 mm event, overestimate would be 10%. Near empty bucket, the respective overestimates are one-half the values given and near full bucket twice the values.

Should one correct for overestimation? For a number of reasons, the answer is no. The temperature coefficients found here are unique to the set of vibrating wire transducers that were used. While all coefficients can be expected to be negative, Fig. 10b shows there are substantial differences in magnitude of the temperature coefficients among the three wires for any given accumulation. Thus it would be necessary to perform a similar type of analysis for each three-wire gauge.

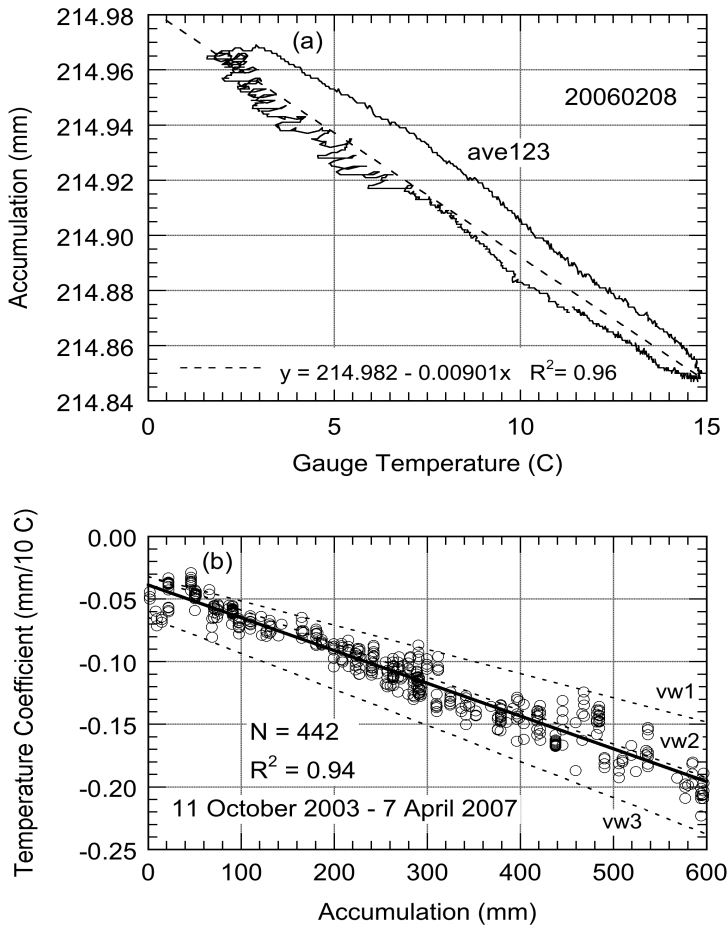


Fig. 10. (a) Plot of accumulation versus temperature in Fig. 9a. The slope of the least-squares linear fit is the temperature coefficient. (b) Temperature coefficients are in units of mm/10°C as a function of accumulation. Dashed lines are least-squares linear fits for individual wires less supporting data. Solid line applies to the average of the three wires with supporting data (open circles)

Undercatch errors due to wind and wetting loss need to be considered, also. Duchon and Essenberg (2001) found undercatch of 4–5% due to wind for both aboveground tipping-bucket and weighing-bucket gauges with and without Alter shields for typical rainfall events across the Southern Great Plains. Clearly, undercatch errors due to wind using an aboveground vibrating wire gauge could easily exceed errors due to temperature.

Golubev et al. (1992) found a 0.03 mm wetting loss for the U.S. standard 8-in rain gauge, but a much higher value for the Tretyakov gauge. Yang et al. (1999) cite a figure of 0.14 mm for the Hellman gauge. In any case, wetting losses depend on both the type of gauge and type of precipitation (Yang et al. 1998). The author is unaware of any such determination for the Geonor gauge.

In conclusion, while there can be a close relationship between accumulation (apparent) and gauge temperature as shown in Fig. 9a, numerically accounting for the magnitude of overestimation in a typical precipitation event is not recommended. Fortunately, this overestimation is counteracted by the undercatch due to wetting loss and wind.

2.7 Rain rate estimation

The availability of a continuous record of gauge-measured 1-min accumulations of precipitation allows for easy calculation of the rate of snowfall or rainfall. In this Section, we examine a heavy rain event in which a two-dimensional video disdrometer or 2dvd, mentioned in Sect. 2.3, provided independent estimates of rain rate. In brief, with the aid of lamps, mirrors and slit plates, two orthogonal video cameras record front and side views of each hydrometeor that falls through a 10 cm \times 10 cm plane located below the 25 cm \times 25 cm orifice seen in Fig. 4. Software is used to match and process the images from each video camera so that drop shape, size, oblateness and fall speed for each drop can be determined. Rain rate is computed from these variables. Much more detail on the operation of the 2dvd can be found in Kruger and Krajewski (2002) and Schuur et al. (2001).

Figure 11 shows a heavy rain event at the field site as measured by the Geonor gauge, the 2dvd and the Oklahoma Mesonet gauge at Norman (NRMN), located 105 m WNW of the pit. The Geonor recorded the most rainfall, the 2dvd the least. The totals for the day were Geonor 100.20 mm, 2dvd 95.97 mm and NRMN 97.28 mm. Note that both the Geonor gauge and 2dvd yield 1-minute data while NRMN gauge yields 5-minute measurements. Two periods A and B in Fig. 11 were selected for rain rate analysis. The former includes the highest rain rates of the event; the latter, the lowest.

Rain rate for the Geonor was calculated by subtracting the previous from the current 1-minute accumulations. Rain rate from the

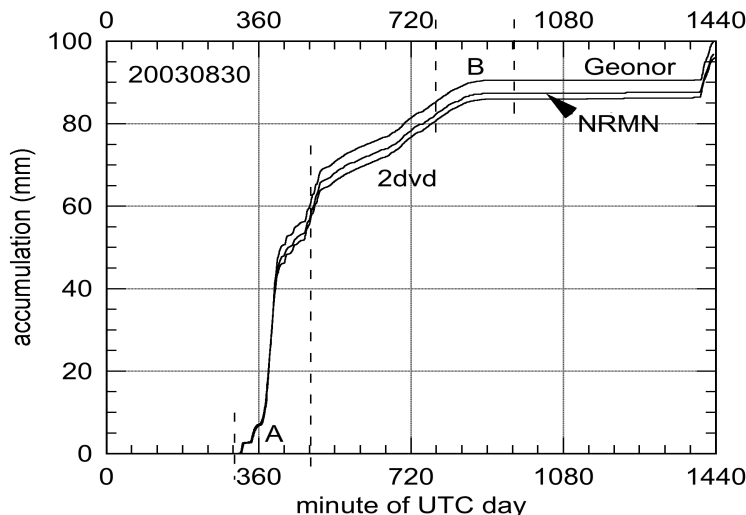


Fig. 11. A heavy rain event. Top accumulation curve is the Geonor, middle curve is the nearby Oklahoma Mesonet gauge (NRMN) and the bottom curve is the two-dimensional video disdrometer (2dvd). The Geonor and 2dvd provide 1-minute data, NRMN 5-minute data. Time period A applies to Fig. 12a,b,c and time period B to Fig. 12d,e,f

2dvd is obtained directly. Figure 12 is a comparison of their rain rates for six 60-minute periods, three in period A and three in period B. With the exception of Fig. 12b, the sensitivities among the rain rate axes are related by an order of magnitude. Including the exception, the range in 1-minute rain rates is more than three orders of magnitude.

Figure 12a covers the initial hour of period A and shows two distinct subperiods of rain and a maximum rain rate of about 42 mm/h. The two curves tend to follow each other quite well. The clocks for the Geonor and 2dvd were not synchronized so there could be a discrepancy of 1-minute or more. The possible discrepancy in time and the fact that the P27 instruction (see Sect. 2.3) was used could account for differences in peak rain rates and/or their displacement in time. These potential limitations apply to all panels in this figure. Figure 12b covers the portion of the rain event with the highest rain rates. Values measured by the Geonor exceed 100 mm/h. A systematic disparity is rain rates can be seen between minutes 380 and 404. Because of the design of the 2dvd wherein the sensing planes are located below the orifice, the trajectories of the raindrops can be at such a low angle relative to the

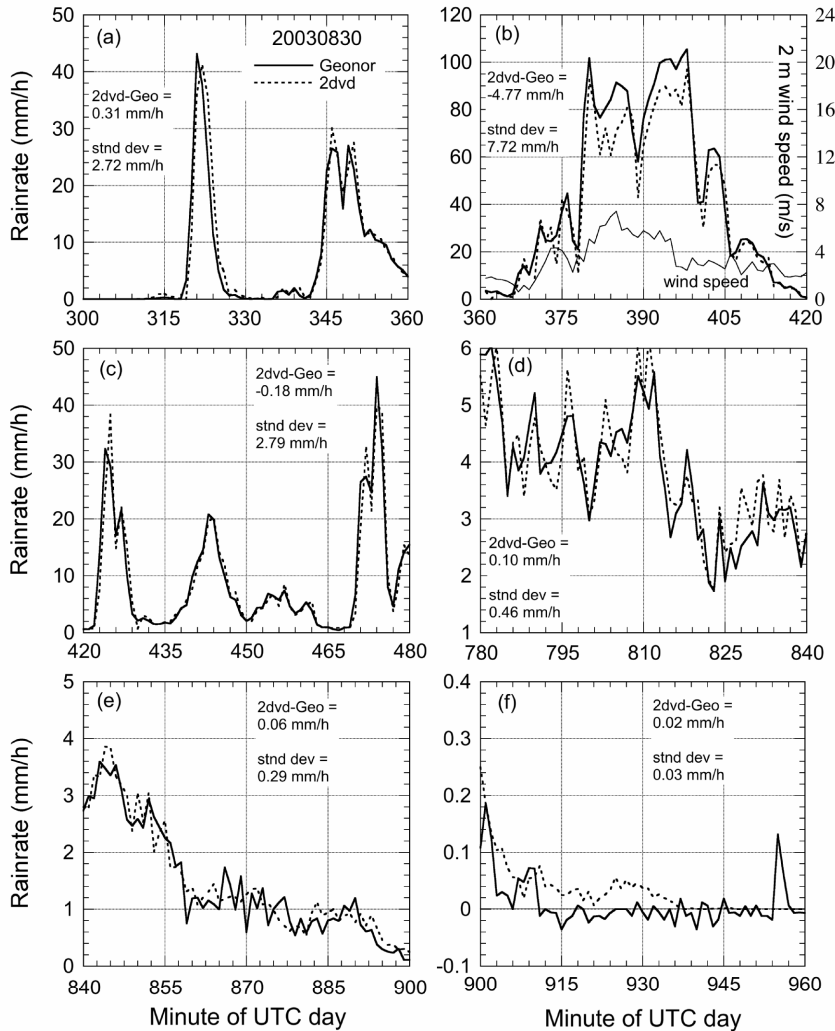


Fig. 12. Comparison of Geonor and 2dvd 1-minute rain rates for periods A and B in Fig. 11. Panels (a), (b) and (c) comprise period A and panels (d), (e) and (f) comprise period B. In (b) the lower curve is wind speed. Note that, with the exception of (b), the sensitivity of rain rate axes can change by an order of magnitude from panel to panel. The mean difference of rain rates and the standard deviation of the differences are shown for each 1-hour period

horizon that there is a ‘shadow effect’ when the wind speed is sufficiently high.

Due to the low trajectory angle, drops may not pass through part of the sensing planes on the windward side. Godfrey (2002, Sect. 3.2)

provides a more detailed explanation. The bottom curve in Fig. 12b shows that the wind speed at 2 m was around or above 4 m/s during this subperiod and may account for the lower rain rates of the 2dvd relative to the Geonor. Figure 12c encompasses the last hour of period A. Correspondence between the two rain rates is good except at the various peaks.

Figure 12d applies to the first hour of period B, the resolution of its ordinate increased by an order of magnitude relative to the previous panel. While the general correspondence between rain rates is satisfactory, differences between their respective peaks and valleys are quite evident.

Rain rates continue to decrease with time in Fig. 12e. When the rain rates decrease to around 1 mm/h, the 2dvd shows a smoother curve than the Geonor. This relationship carries over into Fig. 12f in which the resolution has been increased by another order of magnitude. For values of rain rate less than 0.1 mm/h, the Geonor no longer provides a reliable rain rate as measurement noise dominates beginning about minute 915.

Each figure shows also the mean difference between the 2dvd and Geonor for the associated hour and the standard deviation of the differences. Ignoring Fig. 12b because of the potential bias in the 2dvd due to the wind, a systematic decrease in both the mean differences and standard deviations with decreasing rain rate is observed.

In summary, using the 2dvd as the standard except when wind speed at 2 m exceeds about 4 m/s, the Geonor is capable of measuring 1-minute rain rates with reasonable accuracy from at least 250 mm/h (based on another rain event) down to about 0.1 mm/h (Fig. 12f). With over 1400 gauges world-wide (Sect. 2.1), the opportunity exists to monitor potential changes in rain rates due to a changing climate.

2.8 Very low precipitation events

Because the vibrating wires in the Geonor gauge are sensitive to small changes in tension, it is possible to record trace amounts of precipitation. There are many examples of the occurrence of event totals less than 0.2 mm available in the archived data dating back to 2001. In this Section, four events are discussed that characterize the capability of and the problems associated with estimating trace amounts of rain. No snow events are considered, but, in principle, similar characterizations should apply. The four events are shown in Fig. 13. In each case a

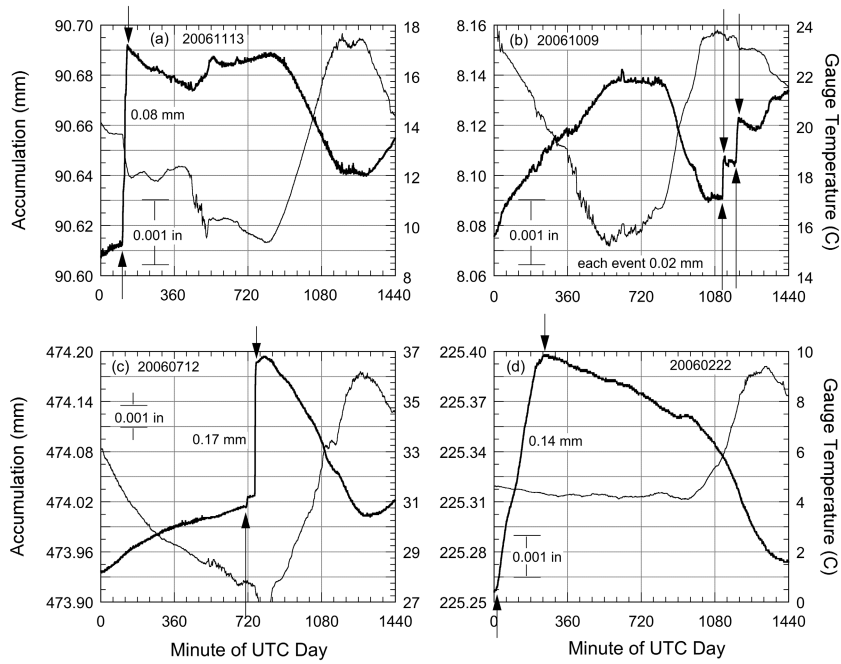


Fig. 13. Accumulation and gauge temperature for four examples of low rainfall events versus minute of a UTC day. Upward and downward pointing arrows define each period of rain. Scale resolution for accumulation in (c) is one-third that in (a) or (b) and in (d) is twice that in (c). Scale resolution for temperature is the same in all panels

comparison is made with the amount observed from the Mesonet gauge and in one case from the 2dvd, also.

Figure 13a shows an event during a UTC day in which 0.08 mm was recorded over a span of 25 minutes. In each panel the time of rainfall is delineated by the upward and downward pointing arrows. Shortly after the rain ends the accumulation decreases slightly as a consequence of evaporation of droplets that failed to penetrate the oil layer and are lying on the oil surface. There is no significant change in temperature for about 5 hours following the event. After about minute 450 there is an increase in apparent accumulation due to a decrease in temperature. Evaporation likely continues for some time but is masked by the response of the vibrating wires to temperature. The second half of the day is characterized by an increase in temperature of 8°C during which time the accumulation decreases by about 0.05 mm. The decrease in accumulation is in agreement with the nominal temperature

coefficient $-0.06 \text{ mm}/10^\circ\text{C}$ seen in Fig. 10b. The NRMN gauge recorded no rainfall, presumably because the rainfall was less than the amount required to tip the bucket, i.e., 0.25 mm.

The first 18 hours of the day in Fig. 13b show the effect of the negative temperature coefficient on (apparent) accumulation. Then beginning at minute 1117 there is a 5-minute shower and at minute 1184 a 10-minute shower, each with a recorded accumulation of 0.02 mm. It is easy to identify even minor shower activity because of the sudden change in accumulation relative to the slowly varying apparent accumulation in response to the daily cycle of temperature. However, the magnitudes of rainfall in both panels (a) and (b) are likely substantial underestimates of the amounts that actually fell due to wetting losses discussed in Sect. 2.6.

Figure 13c shows the results from a day in which three independent estimates of rainfall were available. The accumulation scale is one-third as sensitive as in panels (a) and (b). The Geonor measured 0.17 mm, the Mesonet gauge 0.25 mm and the 2dvd 0.37 mm. The time series of accumulation from the 2dvd matches that of the Geonor along the time axis (not shown), but the amplitudes of the both rain showers are larger. That the Mesonet tipping-bucket gauge shows one tip may be a consequence of residual rain remaining in the bucket from the previous day. Of course, the Mesonet gauge also suffers from wetting loss. Tipping-bucket gauges measure precipitation in discrete amounts and are not useful for measuring very low rainfall events. It seems unlikely that the wetting loss associated with the Geonor could, by itself, account for the difference of 0.20 mm between it and the 2dvd. As cautioned by Kruger and Krajewski (2002, p. 607), the actual size of drops can be overestimated or underestimated depending on whether the 2dvd is properly calibrated. It is the integration of the drop volumes that results in the accumulation estimate. In short, the comparatively large difference between the accumulations from the Geonor and 2dvd remains unexplained.

Following the second rain shower, the gauge temperature reaches a minimum (27°C), then increases to its maximum for the day (36°C), corresponding to an increase of 9°C . During this time the apparent accumulation decreases by 0.18 mm. From Fig. 10b the temperature coefficient is around $-0.17 \text{ mm}/10^\circ\text{C}$ for the given accumulation in the bucket. Thus the observed decrease in accumulation is in line with that expected as a result of the temperature increase; however, evaporation is also likely part of the decrease.

Figure 13d is an unusual case of precipitation in which there is continuous mist for a period of almost 4 hours starting shortly after the

day began. The total accumulation was 0.14 mm (the accumulation scale is twice as sensitive as in panel (c)). The Mesonet gauge recorded 0.25 mm (one tip), but is unreliable because the Mesonet time series suggests it is the last tip of a sequence of tips resulting from melting snow in the gauge (it is unheated). No 2dvd data were available. Evaporation began at about minute 240 and continued for at least the next 11 hours. Evaporation is evident because there is negligible temperature change (sky cover is overcast). At around minute 900 the accumulation remains steady for about one and one-half hours and then continues to decline as the sky cover changes from broken to scattered to clear (based on data from a nearby National Weather Service Automated Surface Observing System station). The data record shows that there was a decrease in gauge temperature of 0.3°C from minute 820 to minute 950, which can be seen in the figure, so that, perhaps, decreasing accumulation due to evaporation was being compensated by increasing accumulation (apparent) due to decreasing temperature, thus yielding an essentially flat accumulation. In addition, the increase in temperature from minute 950 to the maximum for the day is approximately 5°C , which, from Fig. 10b, would result in a decrease in apparent accumulation of 0.05 mm. That the actual decrease from minute 950 to the end of the day is more than 0.08 mm suggests evaporation was occurring simultaneously.

In conclusion, the Geonor vibrating wire gauge is capable of easily measuring increases in accumulation as low as 0.01 mm (see Fig. 13c). Interpreting this amount as the true precipitation is confounded by the wetting loss on the interior wall of the collection cylinder and subsequent evaporation. The magnitude of this loss may well exceed the recorded accumulation, but no definitive analysis has been done, insofar as is known, for either liquid or solid precipitation. Thus careful examination of a time series of accumulation can show that a very small amount of precipitation has occurred and when, albeit the amount is likely an underestimate. Occurrence and timing information can be useful for both meteorological and climatological applications. Simultaneous recording of gauge temperature is an important tool in making the proper assessment of very low precipitation events.

2.9 Summary

The Geonor T-200B vibrating wire precipitation gauge is a sensitive instrument for measuring liquid and solid forms. All analyses presented in this research were based on measurements acquired from a Geonor gauge located in a pit at a field site in central Oklahoma, USA. Because

frozen precipitation seldom occurs in this area and a pit gauge is not suited to measuring snow, only observations of the liquid form were considered. Various aspects of gauge performance have been investigated including (1) advantages of employing three vibrating wires, (2) stability of vibrating wire calibration, (3) the sensitivity of vibrating wire frequency to temperature and (4) application of vibrating wire measurements to a wide range of rain rates and to very low precipitation events.

The redundancy afforded by using three wires can be exploited to build confidence in measurements or to detect poor performance in one or more wires. In addition, using three wires allows one to average their outputs so that random noise due to wind is reduced. Changes in calibration can be detected by placing a succession of known weights into the bucket and observing the output. No significant change in calibrations of the three wires was found over a three-year period. Temperature coefficients are negative and those for the averaged output or accumulation ranged from around $-0.05 \text{ mm}/10^{\circ}\text{C}$ at empty bucket to about $-0.20 \text{ mm}/10^{\circ}\text{C}$ at full bucket (600 mm), a four-fold change.

Correcting accumulation for temperature change is not recommended because, in general, the correction is small and also dependent on the specific wires employed. In very low precipitation events, however, it may be necessary to invoke temperature considerations to make sure the measured accumulation change is not a result or partial result of a temperature change. Comparisons of rain rates from a disdrometer with those from the Geonor generally show close correspondence from very low rain rates to very high rain rates.

In conclusion, the Geonor gauge is a state-of-the-art instrument for accurate and reliable measurement of point precipitation continuous in time.

Acknowledgements

The author wishes to express his many thanks to various members of the Oklahoma Climatological Survey under the direction of Kenneth C. Crawford. They include David Grimsley, Chris Fiebrich, David Demko, and Derek Arndt, who graciously provided a wide variety of technical advice and assistance as well as data management resources. Terry Schuur was kind enough to provide various 2dvd data sets and personal support for this project.

References

- Bakkehøi S, Øien K, Førland EJ (1985) An automatic precipitation gauge based on vibrating-wire strain gauges. *Nord Hydrol* 16:193–202
- Duchon CE, Essenberg GR (2001) Comparative rainfall observations from pit and aboveground rain gauges with and without wind shields. *Water Resour Res* 37:3253–3263
- Godfrey CM (2002) A scheme for correcting rainfall rates measured by a 2-D video disdrometer. MSc Thesis, University of Oklahoma, Norman, USA, 119 pp
- Golubev VS, Groisman PY, Quayle RG (1992) An evaluation of the United States standard 8-in. nonrecording raingauge at the Valdai Polygon, Russia. *J Atmos Ocean Tech* 9:624–629
- Groisman PY, Legates DR (1994) The accuracy of United States precipitation data. *B Am Meteorol Soc* 75:215–227
- Kruger A, Krajewski WF (2002) Two-dimensional video disdrometer: a description. *J Atmos Ocean Tech* 19:602–617
- Lamb HH, Swenson J (2005) Measurement errors using a Geonor weighing gauge with a Campbell Scientific Datalogger. In: *Proceedings 16th Conference on Climate Variability and Change*. American Meteorological Society, San Diego, CA, Paper P2.5
- Raichel DR (2006) *The science and applications of acoustics*. Springer, New York, 660 pp
- Schuur TJ, Ryzhkov AV, Zrnić DS, Schönhuber M (2001) Drop size distributions measured by a 2d video disdrometer: comparison with dual-polarization radar data. *J Appl Meteorol* 40:1019–1034
- Tunbridge LW, Øien K (1988) The advantages of vibrating-wire instruments in geomechanics. *Field Measurements in geomechanics* In: Sakurai S (ed) *Proceedings 2nd International Symposium on Field Measurements in Geomechanics*. 6–9 April 1987, Kobe, Japan. Balkema A.A. Publishers, Brookfield, VT pp 3–16
- Yang D, Goodison BE, Ishida S (1998) Adjustment of daily precipitation at 10 climate stations in Alaska: application of World Meteorological Organization intercomparison results. *Water Resour Res* 34:241–256
- Yang D, Ishida S, Goodison BE, Gunther T (1999) Bias correction of daily precipitation measurements for Greenland. *J Geophys Res* 104:6171–6181

Precipitation: Advances in Measurement, Estimation
and Prediction

Michaelides, S.C. (Ed.)

2008, XXX, 540 p., Hardcover

ISBN: 978-3-540-77654-3